Systematic and Applied Microbiology 47 (2024) 126516

Contents lists available at ScienceDirect

Systematic and Applied Microbiology

journal homepage: www.elsevier.com/locate/syapm

Schauerella fraxinea gen. nov., sp. nov., a bacterial species that colonises ash trees tolerant to dieback caused by *Hymenoscyphus fraxineus*

Undine Behrendt [a,*], Valentin Burghard [a], Sonja Wende [a], Kristina Ulrich [b], Jacqueline Wolf [c], Meina Neumann-Schaal [c], Andreas Ulrich [a,*]

[a] Leibniz Center for Agricultural Landscape Research (ZALF), Microbial Biogeochemistry, Eberswalder Str. 84, D-15374 Müncheberg, Germany
[b] Johann Heinrich Von Thünen Institute, Institute of Forest Genetics, Eberswalder Chaussee 3a, 15377 Waldsieversdorf, Germany
[c] Research Group Bacterial Metabolomics, Leibniz Institute DSMZ - German Collection of Microorganisms and Cell Cultures GmbH, Braunschweig, Germany

ARTICLE INFO

Keywords:
Schauerella fraxinea gen. nov., sp. nov., plant-associated bacteria
Phyllosphere
Fraxinus excelsior
Antagonistic activity
Phylogenomic analysis

ABSTRACT

The tolerance of ash trees against the pathogen *Hymenoscyphus fraxineus* seems to be associated with the occurrence of specific microbial taxa on leaves. A group of bacterial isolates, primarily identified on tolerant trees, was investigated with regard to their taxonomic classification and their potential to suppress the ash dieback pathogen. Examination of OGRI values revealed a separate species position. A phylogenomic analysis, based on orthologous and marker genes, indicated a separate genus position along with the species *Achromobacter aestuarii*. Furthermore, analysis of the ratio of average nucleotide identities and genome alignment fractions demonstrated genomic dissimilarities typically observed for inter-genera comparisons within this family. As a result of these investigations, the strains are considered to represent a separate species within a new genus, for which the name *Schauerella fraxinea* gen. nov., sp. nov. is proposed, with the type strain B3P038^T (=LMG 33092 ^{T} = DSM 115926 ^{T}). Additionally, a reclassification of the species *Achromobacter aestuarii* as *Schauerella aestuarii* comb. nov. is proposed.

In a co-cultivation assay, the strains were able to inhibit the growth of a *H. fraxineus* strain. Accordingly, a functional analysis of the genome of *S. fraxinea* B3P038^T revealed genes mediating the production of antifungal substances. This potential, combined with the prevalent presence in the phyllosphere of tolerant ash trees, makes this group interesting for an inoculation experiment with the aim of controlling the pathogen in an integrative approach. For future field trials, a strain-specific qPCR system was developed to establish an efficient method for monitoring the inoculation success.

Introduction

Ash dieback, induced by the invasive fungal pathogen *Hymenoscyphus fraxineus* (Baral et al., 2014; Kowalski, 2006), has emerged as a significant threat to the ash species *Fraxinus excelsior* L. and *Fraxinus angustifolia* Vahl, along with their associated ecosystems. The disease is spreading rapidly and is presently found in most parts of the European range of ash trees, resulting in a drastic decline in native trees (Enderle et al., 2019; George et al., 2022).

Currently, no effective treatments or methods for controlling the disease are available (Shamsi et al., 2022). Various approaches are being investigated to conserve the common ash as a native forest tree species, including different control, breeding and silvicultural strategies (Langer et al., 2022; Skovsgaard et al., 2017; Tiley and O'Hanlon, 2022). At present, the primary emphasis is on conserving and propagating trees that exhibit tolerance (Enderle et al., 2019). Furthermore, great opportunities are seen in the biological control of the pathogen as an accompanying measure. Studies on the leaf microbiome have revealed a significant association between *H. fraxineus* infection intensity and the composition of ash leaf fungal and bacterial communities (Griffiths

Abbreviations: **AAI, average amino acid identity**; **ANI, average nucleotide identity**; **dDDH, digital DNA-DNA hybridization**; **TYGS, Type (Strain) Genome Server**; **OGRI, overall genome relatedness indi-ces**; **MALDI-TOF MS, matrix-assisted laser desorption/ionization time of-flight mass spec-trometry**; **ASVs, exact amplicon sequence variants**.

* Corresponding authors.
E-mail addresses: ubehrendt@zalf.de (U. Behrendt), Valentin.Burghard@zalf.de (V. Burghard), Sonja.Wende@zalf.de (S. Wende), k.ulrich@thuenen.de (K. Ulrich), jacqueline.wolf@dsmz.de (J. Wolf), meina.neumann-schaal@dsmz.de (M. Neumann-Schaal), aulrich@zalf.de (A. Ulrich).

https://doi.org/10.1016/j.syapm.2024.126516
Received 31 January 2024; Received in revised form 6 May 2024; Accepted 8 May 2024
Available online 12 May 2024

et al., 2020; Ulrich et al., 2020). These results indicate plant beneficial effects of components within the colonising microbial community, which may contribute to defence against the pathogen possibly through direct antagonism, competition, or plant-promoting metabolic activities. Thus, several endophytic fungi of ash trees have been identified in cultural studies that inhibit the growth or germination of *H. fraxineus* and therefore could be used as potential biocontrol agents (Barta et al., 2022; Bilański and Kowalski, 2022; Haňáčková et al., 2017; Kowalski and Bilański, 2021; Schlegel et al., 2016). However, studies under *in planta* conditions have to be performed to confirm these inhibitory effects. Investigations of the bacterial community in tolerant and susceptible ash trees revealed a significantly higher abundance of several bacterial groups, belonging to the genera *Luteimonas* and *Aureimonas*, in the microbiome of tolerant ash trees (Ulrich et al., 2020). Moreover, several bacterial isolates, belonging to genera such as *Bacillus*, *Pantoea* and *Pseudomonas*, exhibited significant growth inhibition of the fungal pathogen in co-cultivation experiments (Ulrich et al., 2020). Inoculation tests with these promising candidates on ash seedlings exposed to the pathogen in the greenhouse confirmed a positive impact on plant health for some of these strains (Becker et al., 2022; Ulrich et al., 2022). This effect seems to be due to a direct antagonistic activity for some strains, while others seem to mediate a colonisation resistance to trigger a priming effect of plant defences against the pathogen.

In the context of these studies, one group of bacteria was isolated that also occurs more frequently in tolerant trees, suggesting that it may be involved in the suppression of ash dieback. Consequently, they are of interest for further investigations to assess their potential in controlling the pathogenic fungus. Phylogenetic studies, initially based on sequence comparisons of the 16S rRNA gene, revealed a relationship with the genus *Achromobacter* (Ulrich et al., 2020). *Achromobacter* species are widespread in the microbiome of plants and involved in various microbe-plant interactions (e.g. Deyett et al., 2017; Raj et al., 2019; Tkacz et al., 2015; Dong et al., 2018). Various strains are capable of modulating concentrations of multiple plant hormones in soils and plants, thereby significantly influencing plant growth (Abdel-Rahman et al., 2017; Nascimento et al., 2021; Santana et al., 2022). Furthermore, certain strains also exhibit activity against fungal pathogens. A strain affiliated with the species *Achromobacter xylosoxidans* suppressed the mycelial growth and conidial germination of *Fusarium solani*, the agent causing common bean root rot disease, both *in vitro* and under greenhouse conditions (Mohamadpoor et al., 2022). Another example is the biocontrol of *Rhizoctonia solani*, the causative agent of fenugreek root rot, under greenhouse and natural field conditions (Rashad et al., 2022).

In this study, we describe a group of strains related to the genus *Achromobacter*, isolated from the phyllosphere of tolerant *F. excelsior* trees. Due to its specific colonisation of tolerant trees, the isolate group could have some potential in suppression of ash dieback. Comprehensive phylogenomic and physiological analyses of these strains were performed to determine their exact taxonomic position. In a co-cultivation assay, the potential of this strain group to inhibit the growth of *H. fraxineus* was investigated. A functional analysis of the genome was conducted to reveal features putatively involved in suppressing the growth of pathogenic fungi. Finally, for future greenhouse experiments and field trials, a strain-specific qPCR system was developed to establish an efficient method for monitoring the success of inoculation through specific quantification.

Materials and methods

Sampling, microbiome analysis by amplicon sequencing and MALDI-TOF MS

Field sampling was conducted in July 2017 at four ash forest districts in Northeast Germany with a severe infestation of *H. fraxineus* infection. In each of the districts, four pairs of adjacent trees consisting of an affected and a tolerant tree were chosen for sampling. Details of the sampling campaign and sample preparation were described previously (Ulrich et al., 2020). In the study of Ulrich et al. (2020) a comprehensive microbiome analysis by amplicon sequencing and MALDI-TOF MS was performed. Based on this data a bacterial group with an increased occurrence on tolerant trees was selected for detailed investigations.

Isolation,** cultivation **and 16S rRNA gene analysis of selected isolates

The isolates were obtained from tolerant trees without visible symptoms in the following districts: B3P038^T from plot B in Karnin (54°15′25.9″N, 12°52′12.5″E), A4P071 from plot A in Lendershagen (54°14′42.1″N, 12°50′31.0″E) and C4P045 from plot C in Pennin (54°15′15.8″N, 13°00′38.6″E). The strains were isolated from a bulked leaf sample of a plot using a method that enable the cultivation of both epi- and endophytic bacteria (Ulrich et al., 2020).

A rough taxonomic classification was performed by sequencing of almost the complete 16S rRNA gene. Total DNA extraction, amplification of the 16S rRNA gene using primers 8f and 1525r and sequencing with internal primers was performed as described by Ulrich et al. (2008). Pairwise comparison of the 16S rRNA gene sequences was conducted on the EzBioCloud platform (Yoon et al., 2017). The 16S rRNA gene sequences for the isolates B3P038^T, A4P071 and C4P045 were deposited in NCBI under the accession numbers OR531683-OR531685.

Genome sequencing

The isolates were cultured in nutrient broth (Roth) for 16 h at 28 °C. Cells were washed twice with ¼-strength Ringer's solution and genomic DNA was then extracted using the Genomic-Tip 100/G kit (Qiagen) according to the manufacturer's instructions. The purity, fragment size and quantity of the isolated DNA were assessed on a 0.7 % agarose gel and by using a NanoDrop ND-1000 spectrophotometer (Thermo Scientific). Genomic DNA of the isolates was used for library preparation and 150 bp paired-end sequencing with an Illumina NovaSeq 6000 sequencer at Eurofins Genomics. Adapter removal was performed using cutadapt v3.4 (Martin, 2011) and bbnorm v38.79 was used to normalize to a target kmer depth of 100x with kmer-size 27. Normalized sequence reads were *de novo* assembled using SPAdes v. 3.15.5 (Vasilinetc et al., 2015) using the "–isolate" option, and the quality assessment of the assembly was done using QUAST 5.0.2. The sequencing projects were deposited in the GenBank database under accession nos. JAVDKK000000000, JAVDKM000000000 and JAVDKL000000000. The assembly statistics and annotation details are given in Table S1.

***Genome analysis and** phylogenomics*

The genome sequences of the isolates were annotated with Rapid Annotation using Subsystem Technology (RAST) version 2.0 (Aziz et al., 2008; Overbeek et al., 2014) and by the NCBI prokaryotic genome annotation pipeline (Li et al., 2021). Functional and pathway analyses were performed using the BlastKOALA web tool of the KEGG database (Kanehisa et al., 2016).

For the phylogenomic analysis, clustering was initially performed using GTDB-Tk v. 2.3.2 (Chaumeil et al., 2022). The analysis of 120 bacterial marker genes resulted in a concatenated amino acid sequence alignment, which was used to calculate a maximum-likelihood tree (LG substitution model with F + G + I) with MEGA (Behrendt et al., 2019). The same set of genome sequences were also used to study the orthologous genes. Prodigal v2.6.3 (Hyatt et al., 2010) was applied to predict protein-coding genes from all genome sequences and orthogroups were identified using the Multiple Sequence Alignment species tree method by OrthoFinder v2.5.5 (Emms and Kelly, 2019) and DIAMOND v2.0.15.153 (Buchfink et al., 2015). As a result, OrthoFinder assigned 97.3 % of total genes from the 104 genome sequences to 15,213 orthogroups. 561 orthogroups consisted entirely of single-copy genes and were present in at least 95.2 % of all species. These 561 genes were the basis of a core

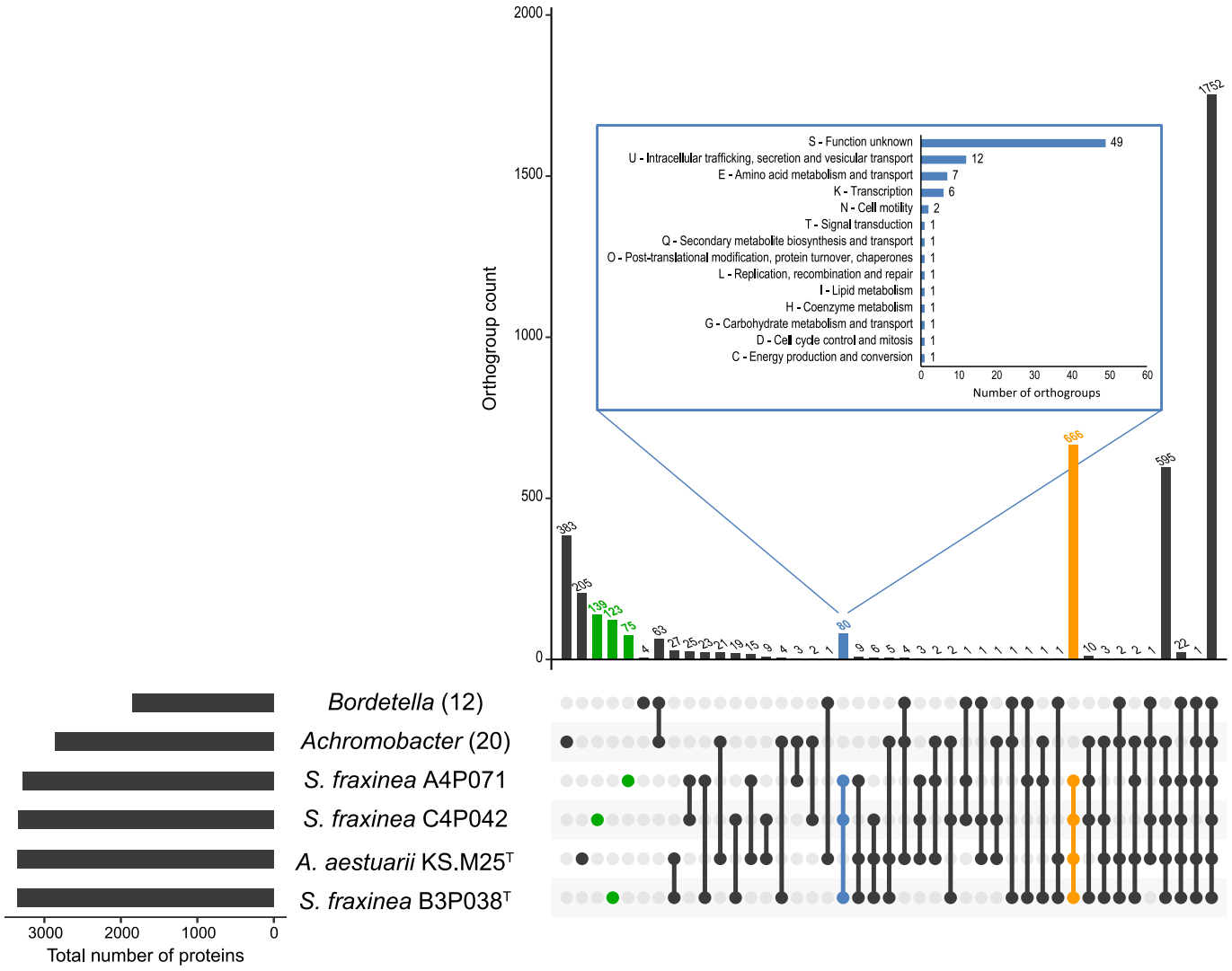

Fig. 1. Orthology analysis of proteins from genomes of the strains B3P038^T, C4P045, A4P071, *Achromobacter aestuarii* KS-M25^T and the core proteome of the genus *Achromobacter* and *Bordetella*. The core proteome is defined as the set of proteins from orthologous genes present in 90 % of the type strains within the genus (number of species is given in brackets). The number of orthogroups for each genome or core proteome is represented by the bar graph in the bottom left. The various intersections are illustrated in the ball-and-stick diagram, and the size of the respective intersection is indicated by the bar graph above. Orthogroups specific to each of the isolated strains, are highlighted in green. Orthogroups that are shared by the strain group and the closely related species *A. aestuarii* are shown in orange. Orthogroups specific for the strain group are coloured in blue and the inset bar chart shows their classification to functional COG categories. Abbreviations: *S.*, *Schauerella*; *A.*, *Achromobacter*.

genome phylogeny approach. The concatenated amino acid sequence alignment of the genes were provided as input into IQ-TREE v1.6.12 (Nguyen et al., 2015) using default parameters. The substitution model used was LG + F + G + I, identified as the best-fit model by the ModelFinder program (Kalyaanamoorthy et al., 2017), and 100 non-parametric bootstrap replicates were calculated to determine branch support. Both trees were visualised and rooted with MEGA.

The number of shared orthogroups across selected strains and related genera was illustrated as UpSet plots using the R package UpSetR 1.4.0 (Conway et al., 2017). For genera harbouring more than one species, core orthogroups of the genus were defined as orthogroups present in at least 90 % of the species. Orthogroups of special interest were further annotated using EggNOG-mapper (Huerta-Cepas et al., 2017).

The average nucleotide identity (ANI) values were calculated using OrthoANIu v1.2 (Yoon et al., 2017) which employees USEARCH (Edgar, 2010) for the comparisons. Furthermore, gANI and the alignment fraction (AF) were calculated for a pair of genomes by averaging the nucleotide identity of orthologous genes using ANIcalculator as defined by Varghese et al. (2015). Mean values of the reciprocal pairwise comparisons were plotted in Fig. 4.

Digital DNA-DNA hybridization (dDDH) and genomic G + C content were determined using the Type Strain Genome Server (TYGS; Meier-Kolthoff and Göker, 2019). To support the taxonomic classification, average amino acid identity (AAI) as a further genome relatedness index was calculated using EzAAI v1.1 (Kim et al., 2021).

Ecological significance

To gain an understanding of the distribution, abundance, and genetic similarity of the taxon under investigation, a screening was conducted using public databases. The full 16S rRNA gene sequence of strain B3P038^T was aligned to the NCBI nt database (database accessed march 2024). The results were filtered to include matches with a percent identity $\geq$ 98.65 and a query coverage $>$ 99, ensuring complete coverage of the 16S rRNA gene sequence. This filtering process yielded 9 matches, for which the original habitat was determined. Additionally, a blast-vdb search through 31 plant metagenomes (taxid: 1297885) and 1281 soil metagenomes (taxid: 410658) in NCBI's wgs data was

Table 1
Overall genome relatedness indices and 16S rRNA gene sequence similarity calculated for the strains B3P038^T, A4P071 and C4P045 in comparison to related species.

Genomes	dDDH values (%)	ANI (%)*	Diff. GC-content (%)	AAI (%)*	16S rRNA
B3P038^T *vs.*					
C4P045	84.0	98.06	0.10	99,06	100.00
A4P071	83.6	98.11	0.11	99,03	100.00
Achromobacter aestuarii KS-M25^T	36.9	88.85	0.37	94.88	99.93
Achromobacter anxifer LMG26857^T	20.7	75.01	4.33	71.38	98.04
Achromobacter veterisilvae LMG 30378 ^{T}	20.7	74.89	5.28	71.19	97.96
C4P045 *vs.*					
A4P071	83.7	98.71	0.00	99.01	100.00
Achromobacter aestuarii KS-M25^T	36.9	88.81	0.26	94.85	99.93
Achromobacter anxifer LMG26857^T	20.7	75.22	4.23	71.56	98.04
Achromobacter veterisilvae LMG 30378 ^{T}	20.7	74.93	5.18	71.29	97.96
A4P071 *vs.*					
Achromobacter aestuarii KS-M25^T	36.9	88.74	0.26	94.87	99.93
Achromobacter anxifer LMG26857^T	20.7	75.12	4.22	71.58	98.04
Achromobacter veterisilvae LMG 30378 ^{T}	20.8	75.22	5.17	71.36	97.96

*A detailed analysis is shown in Table S3.

performed to find matches to the above defined threshold. This search strategy was repeated for a selection of 10 housekeeping genes from strain B3P038^T (*rpsH, rplJ, dnaA, rpoA, rpoB, rpoC, NusA, lepA, rpsI* and *recA*).

Furthermore, the amplicon sequencing data of the bacterial community on ash leaves at different stands in the UK (Griffiths et al., 2020) were analysed for related ASV's. The 16S V4 rRNA sequencing data of 137 samples deposited in the NCBI Sequence Read Archive under project number PRJNA515030 were downloaded. After merging paired reads using pear (Zhang et al., 2013), each sample was compiled as BLAST database using local BLAST+ (v 2.15.0) and searched for the 16S rRNA gene sequence of strain B3P038^T. Matches were filtered for full V4 region alignment, revealing one sample with 13 matches at a percent identity of $\geq$ 98.65. Subsequently, the paired reads of this sample were processed using the DADA2 pipeline as described by (Ulrich et al., 2020). The 13 reads formed a single ASV with a reference sequence showing only one mismatch to the 16S rRNA gene sequence of B3P038^T (99.6 % similarity). After removing plastid and mitochondrial sequences of ash trees from the dataset, the relative abundance of the ASV was calculated.

Phenotypic characterisation

Phenotypic analyses was performed for the strains B3P038^T, A4P071, C4P045 and the reference strain *Achromobacter aestuarii* JCM 33329 ^{T}. Standard methods for morphological and physiological characterisation were conducted as described by Behrendt et al. (1999). Unless otherwise stated, strains were cultivated on nutrient agar II (NAII; Sifin) or in the respective broth at 30 °C. Presence of oxidase was tested on Cytochrome Oxidase Test Strips (Merck). Oxidation of carbon compounds and resistance to inhibitory chemicals were determined using GEN III MicroPlates (Biolog) inoculated with IF-A medium according to the manufacturer's instructions. Results were scored visually after 24 and 48 h incubation at 30 °C. Additional physiological and enzymatic characteristics were determined using the API 20E and API 20NE test strip (bioMérieux) after 48 h incubation at 30 °C. Since none of the strains grew in the GEN III plates at pH 5, the pH tolerance experiment was conducted in the range of pH 6.0–11.0 using the buffer system described by Ngo and Yin (2016). Furthermore, growth was tested at temperatures of 4, 10, 20, 30, 35 and 37 °C and at NaCl concentrations of 0, 0.5 and 1–6 % with 1 % increase.

Analysis of cellular fatty acids was performed after cultivation on tryptic soy broth (TSB) for 1 days at 28 °C. Fatty acid profiles were determined as described by Timsy et al. (2022). Polar lipids were extracted from freeze dried cell material using a choroform:methanol:0.3 % aqueous NaCl mixture and recovered into the chloroform phase [modified after Bligh and Dyer (1959)]. The separation of polar lipids was achieved through two-dimensional silica gel thin-layer chromatography. The first direction was developed in chloroform: methanol:water, and the second in chloroform:methanol:acetic acid: water. Molybdophosphoric acid was employed to detect total lipid material, and specific functional groups were identified using spray reagents designed for defined functional groups (Tindall et al., 2007). Polyamines were extracted from wet biomass following the metabolite extraction protocol outlined by Zech et al. (2009) and subsequently derivatized and analysed using GC–MS as described by Will et al. (2019). Respiratory quinones were extracted from cell material using hexane and purified by a silica-based solid phase extraction. Purified samples were analysed by reversed-phase HPLC coupled to a diode array detector and a high-resolution mass spectrometer (Vieira et al., 2021).

In vitro screening of antagonistic activity toward *h. Fraxineus*

The bacterial isolates were screened for their antagonistic activity toward different *H. fraxineus* strains (7, HF6 and HF8) by a co-cultivation assay described by Ulrich et al. (2020). Briefly, an agar plug with *H. fraxineus* mycelium was placed in the centre of the petri dish, while the tested bacterial isolate was spread around the edge of the plate. Plates containing the *H. fraxineus* mycelium alone were used as control. Due to its slow growth, *H. fraxineus* was inoculated 5 days before the bacteria.

Development of a strain-specific qPCR assay for the strain B3P038^T

Based on the workflow developed by Burghard et al. (2023), a strain-specific qPCR detection system was designed for strain B3P038^T. Briefly, we created a database of all currently known genome sequences within the family *Alcaligenaceae* (322 genomes). All genome assemblies were retrieved from the NCBI database. Neptune v1.2.5 (Marinier et al., 2017) was applied to find the specific sequences by testing the target genome (B3P038^T) against the genomic database. The uniqueness of the sequence with the highest score was confirmed by a BLAST search. The design the primer-probe system was conducted by OligoArchitect™ (Sigma-Aldrich Co, 2014). The oligo sequences of the assay are 5′-cgg ata agt gga tga aga-3′ for the forward primer, 5′-cct agc aga act tga gag-3′for the reverse primer and 5′-agt tcc gtt cca gat tca gtc gt-3′ for the probe. The cycling conditions were 95 °C for 2 min and 40 cycles of 95 °C for 15 sec and 60 °C for 1 min using Luna® Universal Probe qPCR Master Mix (New England Biolabs, Germany). Optimization of the assay resulted in final concentrations of 0.5 µM for both primers and 0.15 µM for the probe. The specificity of the qPCR system was evaluated by testing the related strains C4P045 and A4P071 as well as the type strain of the closely related species *A. aestuarii* (JCM 33329 ^{T}).

Results and discussion

Taxonomic investigation

Strain and species status of the investigated isolates. The representative strains of the isolate group (B3P038^T, C4P045, and A4P071) were

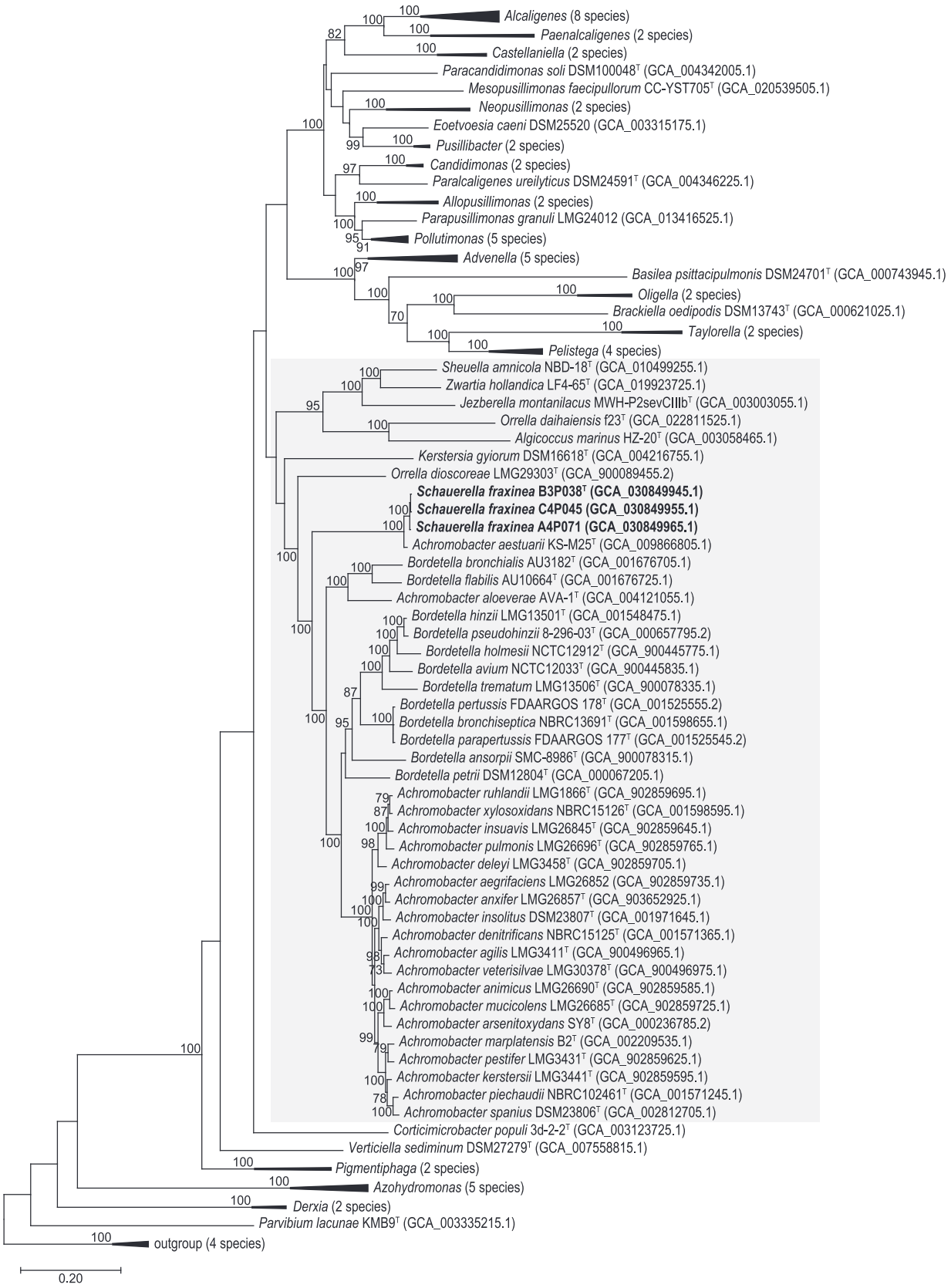

Fig. 2. Phylogenomic tree showing the position of the strains B3P038^T, C4P045, A4P071 among type strains of the family *Alcaligenaceae.* The maximum-likelihood tree is based on concatenated 120 marker proteins. *Burkholderia cepacia* ATCC25416^T, *Burkholderia stagnalis* CCUG65686^T, *Caballeronia glathei* LMG14190^T, and *Caballeronia novacaledonica* LMG28615^T was used as outgroup. Numbers at branch nodes refer to bootstrap values $\geq$ 70 %. Bar: amino acid substitutions per position. Assembly accession numbers are indicated in brackets. The subset of type strains used in further analysis is marked in grey. (Fig. S1, expanded view).

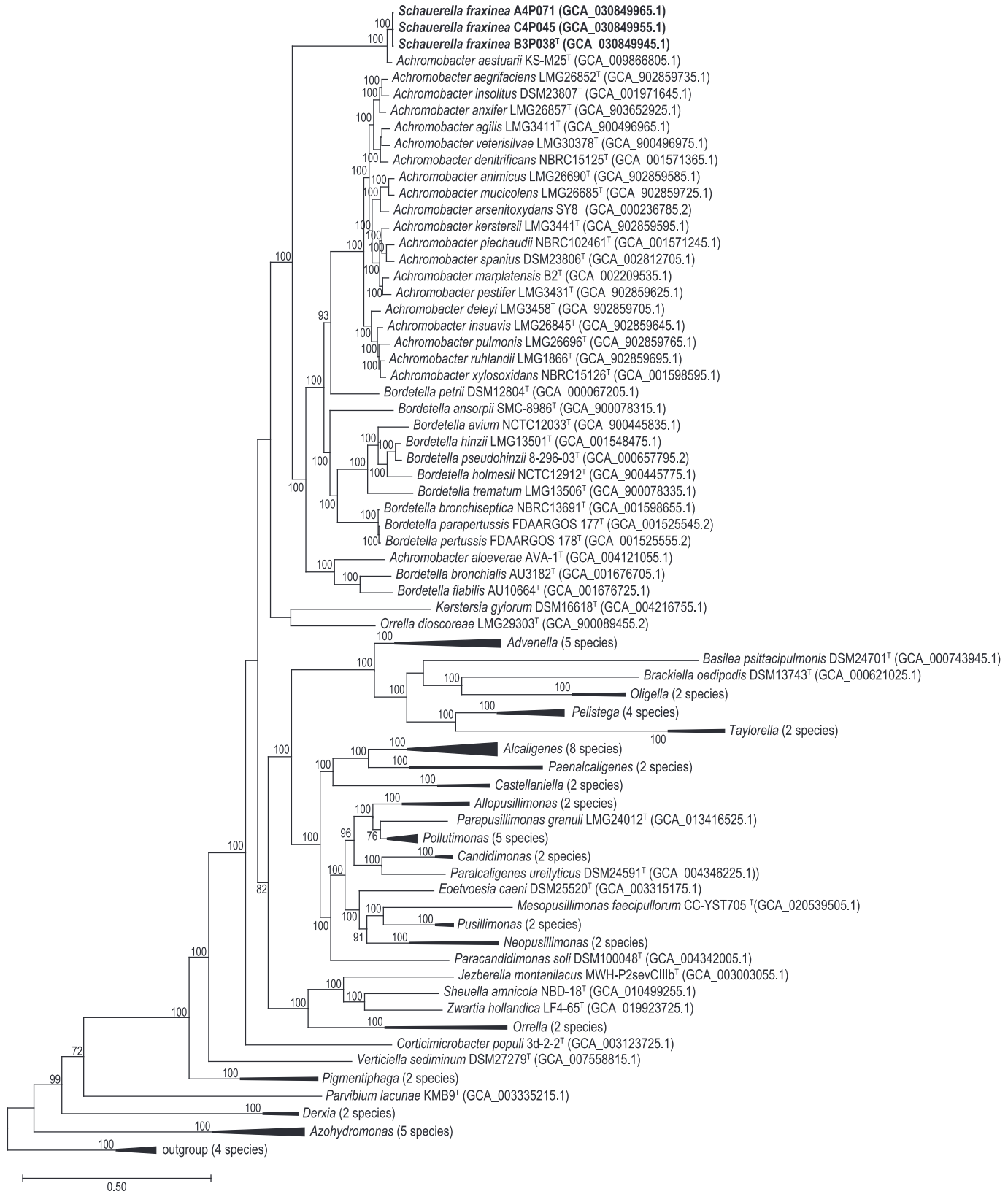

Fig. 3. Phylogenomic tree showing the position of the strains B3P038^T, C4P045, A4P071 among type strains of the family *Alcaligenaceae.* The maximum-likelihood tree is based on concatenated 561 single copy orthologous genes. *Burkholderia cepacia* ATCC25416^T, *Burkholderia stagnalis* CCUG65686^T, *Caballeronia glathei* LMG14190^T, and *Caballeronia novacaledonica* LMG28615^T was used as outgroup. Numbers at branch nodes refer to bootstrap values $\geq$ 70 %. Bar: amino acid substitutions per position. Assembly accession numbers are indicated in brackets. (Fig. S2, expanded view).

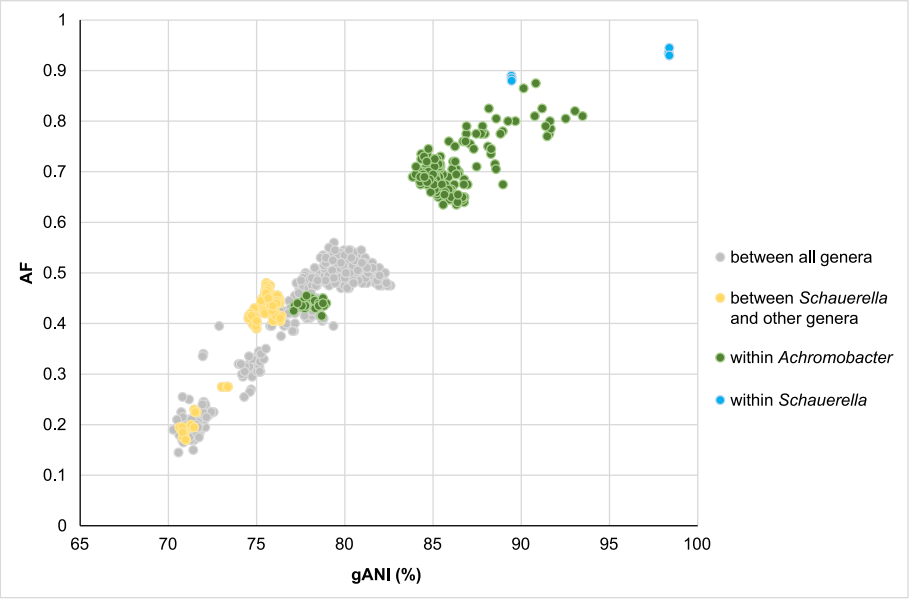

Fig. 4. Ratio of pairwise comparisons of average nucleotide identity (gANI) and alignment fractions (AF) for the subset of type species of the family *Alcaligenaceae* (grey-marked in Fig. 2). Data for within-genus comparisons of *Schauerella* gen. nov. (*S. fraxinea* B3P038^T, C4P045, A4P071, and *A. aestuarii* JCM 33329 ^{T}) and *Achromobacter* as well as intra-genera comparisons for *Schauerella* gen. nov. were highlighted.

selected from different sites to minimize the likelihood of clonality. As a basis for further genomic and phylogenetic analyses, their genomes were sequenced. *De novo* assembly resulted in an almost complete genome sequence of circa 5.4 Mb for each isolate Assembly statistics and annotation details are shown in Table S1. Analysis of orthologous genes revealed several differences among the isolates, confirming their distinct strain status (Fig. 1). Specifically, strains B3P038^T, C4P045, and A4P071 exhibited 123, 139, and 75 proteins, respectively, exclusively found within each strain. Furthermore, variations in the oxidation of the carbon sources D- and L-fucose, glycyl-L-proline, D-lactic acid methyl ester, α-hydroxy butyric acid and acetoacetic acid in the Biolog GEN III test system demonstrated a physiological variability of the group. In contrast, sequencing of the16S rRNA genes resulted in identical sequences. The analysis of overall genome relatedness indices (OGRI) clearly revealed an affiliation to the same species (Table 1). Thus, dDDH resulted in values above the species boundary of 70 % (Meier-Kolthoff et al., 2013). Accordingly, the ANI and AAI values were higher than the recommended species cut-off level of 95 % (Konstantinidis and Tiedje, 2005; Palmer et al., 2020). In addition, the differences in the genomic G + C content were far below 1 % (Meier-Kolthoff et al., 2014).

Phylogenetic position of the strain group. Pairwise 16S rRNA gene sequence comparison revealed a 99.93 % match with the type strain *A. aestuarii* JCM 33329 ^{T}, indicating a close relationship. However, OGRI values below species boundary clearly demonstrated a separate species position of the investigated strains (Table 1). The next closest relationships, based on 16S rRNA gene phylogeny, were with the strains *Achromobacter anxifer* LMG26857^T and *Achromobacter veterisilvae* LMG 30378 ^{T} (Table 1), demonstrating similarities of 98.04 % and 97.96 %, respectively. This was followed by other *Achromobacter* and *Bordetella* species, which also showed similarities higher than 97.0 %. These results suggest a position in the family *Alcaligenaceae* related to the genera *Achromobacter* and *Bordetella*. However, a comparison of 16S rRNA gene sequences between the type species of this family by Hahn et al. (2022) revealed similarities in the range of 97.0 to 98.5 % for several pairs. These unusually high values lead to the conclusion of a relatively slow molecular evolution of the 16S rRNA gene in these genera compared to the protein-encoding part of their genomes. Therefore, the focus of further phylogenetic analyses shifts to genome-based methods. However, it should be noted that for three genera, each represented by one species, no genome sequences are available. 16S rRNA gene comparisons revealed similarity values of 91.4 %, 96.1 %, and 95.4 % for the isolates and the type strains of these species – *Ampullimonas aquatilis* B15.09–116 ^{T}, *Caenimicrobium hargitense* CGII-59m2^T, and *Saccharedens versatilis* CAG32^T, respectively. These relatively low values, combined with their positions in phylogenetic trees (Babich et al., 2023; Hahn et al., 2022), strongly suggest that a close relationship is unlikely.

To gain phylogenomic insights, an analysis of 120 marker genes present in a wide range of bacteria (Chaumeil et al., 2022) was conducted to achieve a deeper understanding of the relationships within the family (Fig. 2, collapsed tree view, and Fig. S1, expanded view). Corresponding to the matches in the 16S rRNA gene sequence, the studied strains and *A. aestuarii* formed a cohesive cluster supported by high bootstrap values. This cluster was located outside a cluster formed by the two genera *Achromobacter* and *Bordetella*. This distinct position was supported by a bootstrap value of 100 %. The next related branch is formed by the type species *Orrella dioscoreae* followed by a separate branch of the type species *Kerstersia gyiorum*, whereas the former is supported by a high bootstrap value. With respect to the investigated strains, this analysis suggested that they would merit a separate genus status along with the species *A. aestuarii*.

To verify this result, a core genome analysis based on orthologous genes was performed (Emms and Kelly, 2019). The phylogenomic tree was calculated with a concatenated protein sequence of 561 single copy orthologous genes (Fig. 3, collapsed tree view, and Fig. S2, expanded view). Again, the isolated strains and *A. aestuarii* formed a separate monophyletic cluster on a branch related to the genera *Achromobacter* and *Bordetella*, which in turn form a joint cluster. A shared cluster of the type species *O. dioscoreae* and *K. gyiorum* formed the next related branch. This constellation was also supported by bootstrap values of 100 %, confirming the results of the first phylogenomic analysis. The separate position of the studied strains together with the species *A. aestuarii*, became even more evident in this phylogenetic tree and supported the assumption of a separate genus status. Thus, the branch length that indicates the phylogenetic distance between this cluster and related genera is longer than many branches connecting other genera of the family *Alcaligenaceae*.

In both trees (Fig. S1; S2), a polyphyly of the related genera *Achromobacter*, *Bordetella* and *Orrella* becomes visible. Especially the species

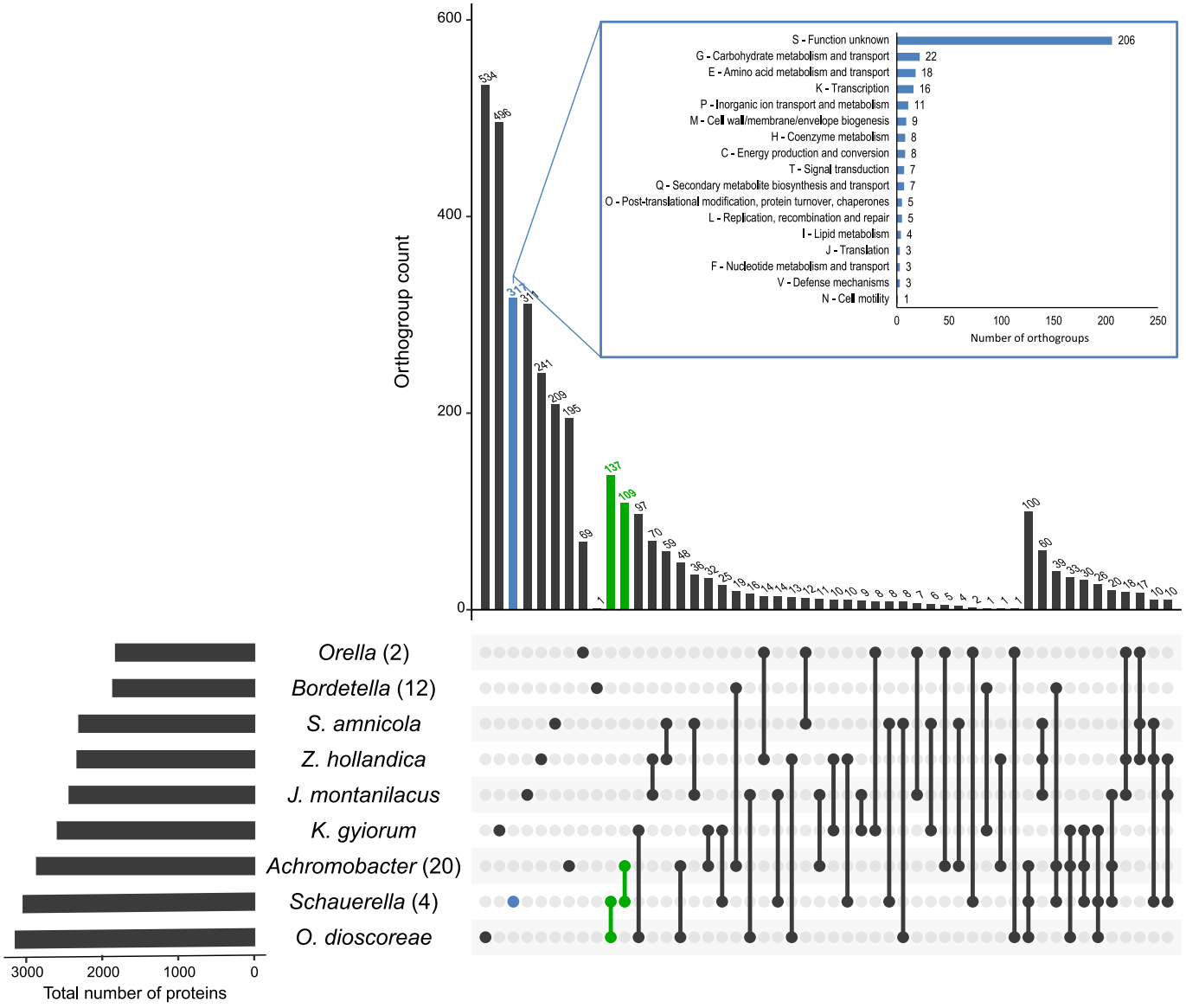

Fig 5. Upset plot comparing shared orthogroups between the core proteome of *Schauerella* gen. nov. (*S. fraxinea* B3P038^T, C4P045, A4P071, and *A. aestuarii* KS-M25^T) and that of related genera (subset grey-marked in Fig. 2). The core proteome is defined as the set of proteins from orthologous genes present in 90 % of the type strains within the genus (number of species is given in brackets). For the genera *Sheuella* (*S.*), *Zwartia* (*Z.*), *Jezberella* (*J.*), and *Kerstersia* (*K.*), the genome for only one type strain/species was available. The genus *Orella* (*O.*) was subdivided in the type species *O. dioscoreae* and the remaining species *O. daihaiensis* and *O. marina*. They were separately analysed because of the significant polyphyly in the phylogenomic analysis. Orthogroups specific to the genus *Schauerella* are highlighted in blue and the inset bar chart shows their classification to functional COG categories. Numbers of orthogroups shared with the related genus *Achromobacter* and *O. dioscoreae* are highlighted in green. The first 50 intersections/overlaps between orthogroups are displayed.

Orrella daihaiensis and *Orrella marina*, formed a cluster far distant from the type species *O. dioscoreae*. A closer look at the taxonomic history of this genus reveals that *O. marina* was originally described by Ying et al. (2019) as the type species *Algicoccus marinus* in a proposed new genus. During the description of the species *Orrella amnicola*, it was reclassified and assigned to the genus *Orrella* (Sheu et al., 2020). More recently, *O. amnicola* found a place in the new genus *Sheuella* (Hahn et al., 2022). However, the classification of *O. marina* by Ying et al. (2019) seems to be more in agreement with the results of this study than that of Sheu et al. (2020), and the correct name should be *Algicoccus marinus*.

However, turning back to the primary focus of this study – the isolated strain group – the OGRI values were analysed to uncover additional evidence supporting a distinct genus status. Comparison of AAI values (Table S2) of the genera *Achromobacter* and *Bordetella* and the type species of *Orrella* revealed values within in the range of 72.4 % (*Bordetella pertussis* FDAARGOS 178 ^{T}) and 68.6 % (*O. dioscoreae* LMG29303^T). In contrast to species differentiation, the AAI value is not as clearly applicable for delimiting genera (Barco et al., 2020). An AAI value of 65 % is suggested as the lower limit for the next taxonomic rank (Konstantinidis and Tiedje, 2007; Konstantinidis et al., 2017). However, due to considerable overlap, AAI values between different genera can fall within the range of 65 % to 95 %. Therefore, it is recommended to adjust the threshold to account for the specificity of candidate taxa (Konstantinidis et al., 2017). Babich et al. (2023) analysed the intra- and inter-genus distribution of AAI values in the family *Alcaligenaceae*. They demonstrated that using a threshold value of approximately 75 % for the separation of genera correlated with the branching of the phylogenomic tree. Considering this value, the analysis of AAI values supports a separate genus position for the isolated strains, along with *A. aestuarii*.

Another parameter used to support genus demarcation within the family *Alcaligenaceae* is the analysis of the gANI to AF ratio (Hahn et al., 2022). Plotting these values (Fig. 4) demonstrated that genomic

Table 2
Fatty acid contents (%) of the strains B3P038^T (1), C4P045a (2), A4P071a (3) and the type strain of the closely related species *Achromobacter aestuarii* JCM 33329 ^{T} (4).

Fatty acid	1	2	3	4
Saturated, straight-chain				
$C_{12:0}$	0.6	0.7	0.6	TR
$C_{14:0}$	4.2	4.7	4.9	1.1
$C_{15:0}$				TR
$C_{16:0}$	23.9	22.1	22.4	22.8
$C_{17:0}$	0.5	0.6	0.5	TR
$C_{18:0}$	2.6	2.5	2.4	2.3
unsaturated				
$C_{15:1}$ *ω6c*	–	TR	TR	TR
$C_{16:1}$ *ω7c*	44.8	45.8	46.6	37.5
$C_{18:1}$ *ω7c*	14.0	11.9	11.3	11.7
11-Methyl $C_{18:1}$ *ω7c*	TR	TR	TR	0.7
hydroxylated				
$C_{12:0}$ 2-OH	2.4	2.7	2.2	2.9
$C_{12:0}$ 3-OH	0.50	0.50	TR	
$C_{14:0}$ 2-OH				2.99
$C_{14:0}$ 3-OH	5.8	6.1	5.7	7.9
others				
$C_{17:0}$ cyclo *ω7c*	TR	1.7	2.3	9.1

TR, trace (<0.5 %). All data were generated in this study.

Table 3
Physiological characteristics distinguishing strains B3P038^T (1), C4P045 (2), A4P071 (3) and the type strain of the closely related species *Achromobacter aestuarii* JCM 33329 ^{T} (4).

Characteristic*	1	2	3	4
Growth at pH 5	+	+	+	–
Oxidation (GEN III) of:				
D-Aspartic Acid	–	–	–	+
Bromo-Succinic Acid	+	+	+	–
β-Hydroxy-D,L Butyric Acid	–	–	–	+
Propionic Acid	–	–	–	+
Resistance (GEN III) to:				
Potassium Tellurite	+	+	w	–

*Data from this study for all strains; +, positive; –, negative; w, weak reaction.

dissimilarities of the studied strain group and *A. aestuarii* fell within the typical range observed for inter-genera comparisons among related genera. An intra-genus comparison of *Achromobacter* revealed, in addition to a core group, a separate subgroup that exhibited typical inter-genera dissimilarities, which are attributed to the genome of the strain *Achromobacter aloevera* AVA-1 ^{T}. This distinct position is further supported by its polyphyletic placement in the phylogenetic trees (Fig. 2; Fig. 3), recommending a taxonomic reassessment. In contrast, the investigated strain group and *A. aestuarii* displayed gANI to AF ratios consistent with those of the core group of *Achromobacter*. Consequently, this analysis supports the joint assignment of the strain group and the species *A. aestuarii* to a new genus.

Finally, as part of the comparative genomic studies, a comprehensive analysis was conducted to examine the distribution of shared and unique orthogroups. The first UpSet plot (Fig. 1) focuses specifically on the differences and intersection of the isolated strains that represent a separate species. The strains of this group shared 80 orthogroups that were not present in the closely related type strain *A. aestuarii* KS.M25^T and not part of the core orthogroups of the genera *Achromobacter* and *Bordetella*. These orthogroups clearly differ the studied strain group from related taxa and delineate functional differences among them at the species level. To gain more insights into the unique properties of the strain group, the species-specific orthogroups were classified into functional categories using the COG database. The vast majority of orthogroups (49) were classified under the 'category S: function unknown', which also includes proteins with a putative function. Apart from this, most orthogroups belonged to category U (intracellular trafficking, secretion and vesicular transport; 12 orthogroups), followed by category E (amino acid metabolism and transport; 7 orthogroups). A further argument for the species delimitation from *A. aestuarii* is the number of unique orthogroups of this species (205), which significantly exceeded the corresponding values in each of the strains examined. Examining the isolated strains together with the species *A. aestuarii*, an intersection of 666 orthogroups was identified, distinguishing them from the genera *Achromobacter* and *Bordetella*. This aspect becomes even more apparent in the second UpSet diagram (Fig. 5) concerning the selected subset of genera within the family *Alcaligenaceae* (Fig. 2). In this context, 317 specific orthogroups were identified within the core orthogroups of the potentially new genus. Classification into functional categories revealed a special genetic makeup, especially in carbohydrate metabolism and transport, amino acid metabolism and transport, as well as inorganic ion transport and metabolism (Fig. 5). This result suggests a genetic basis for phenotypic differences and ecological adaptations at genus level.

In summary, it can be stated that the isolated strains unequivocally merit a position in a distinct species within a new genus. Therefore, we propose the genus *Schauerella* gen. nov., where the isolated strains form the type species *Schauerella fraxinea* sp. nov. Additionally, a reclassification of *Achromobacter aestuarii* described by Kim et al. (2021) as *Schauerella aestuarii* comb. nov. is proposed.

Phenotypic characterisation: While in the past, a comprehensive phenotypic delimitation was required when describing a new species within a polyphasic approach, the current opinion tends to consider a genomic analysis sufficient, especially in species descriptions. (Vandamme and Sutcliffe, 2021). For the description of taxa at a higher level, a chemotaxonomic characterisation is welcomed (Vandamme and Sutcliffe, 2021). However, genera within the family *Alcaligenaceae* cannot be clearly differentiated from each other using these methods (Babich et al., 2023; Vaz-Moreira et al., 2011). Therefore, important chemotaxonomic parameters of the proposed new genus were only described as such within this framework and discussed in the general context of the family.

The analysis of polar lipid patterns revealed the presence of diphosphatidylglycerol, phosphatidylethanolamine and phosphatidylglycerol (Fig. S3), which are also typical for members of several genera in the family (Austin et al., 2014; Babich et al., 2023; Hahn et al., 2022; Vaz-Moreira et al., 2011). Differences were reported in the presence/absence of unknown phospholipids, glycolipids, aminolipids and lipids. The comparison between the new species *S. fraxinea* and *S. aestuarii* revealed differences in the presence of an aminophospholipid, which was identified in each of the isolated strains (Fig. S3). Strain-specific differences became evident with a phospholipid and aminolipid that were absent in the type strain B3P038^T but present in the related strains. In the analysis of the polyamine profiles of both species, putrescine and 2-hydroxyputrescine were identified. This result is consistent with the typical profile of members in the class of Betaproteobacteria, which contain the unusual diamine 2-hydroxyputrescine, putrescine, and occasionally notable levels of spermidine (Abdel-Rahman et al., 2017; Burghard et al., 2023; Huerta-Cepas et al., 2017). Analysis of respiratory quinones revealed Q8 as the predominant ubiquinone for both species, *S. fraxinea* (98.7 ± 0.36 %) and *S. aestuarii* (98.9 %). Only traces (<1%) were determined for the ubiquinone Q7 and Q9, respectively. These results are consistent with the majority of genera in the family *Alcaligenaceae* (Austin et al., 2014). The cellular fatty acid profiles of the isolated strains are very similar to each other, which reflects the affiliation into one species (Table 2). The predominant fatty acids (>10 %) were the saturated acid $C_{16:0}$ and the unsaturated fatty acids $C_{16:1}$ *ω7c* and $C_{18:1}$ *ω7c*. The predominant fatty acids within the family *Alcaligenaceae* include $C_{16:0}$ and $C_{17:0}$ cyclo (Austin et al., 2014), which also applies to the related genus *Achromobacter* and *Bordetella* (Austin et al., 2014; Busse et al., 2006). In contrast, the proportion of the fatty acid $C_{17:0}$ cyclo *ω7c* was rather low in the genus *Schauerella.* However, significant differences were observed between the species *S. fraxinea* (1.4

Table 4
Description of the new genus *Schauerella* including the species *Schauerella fraxinea* sp. nov. and an emended description of *Schauerella aestuarii* comb. nov.

Guiding Code for Nomenclature [req]	ICNP	ICNP	ICNP
Nature of the type material	Strain	Strain	Strain
Genus name	*Schauerella*	*Schauerella*	*Schauerella*
Species name	–	*Schauerella fraxinea*	*Schauerella aestuarii*
Genus status	gen. nov.	–	–
Genus etymology	Schau.e.rel'la. N.L. fem. dim. n. *Schauerella,* named in honour of the German microbiologist Frieder Schauer	–	–
Type species of the genus	*Schauerella fraxinea*	–	–
Specific epithet	–	*fraxinea*	*aestuarii*
Species status	–	sp. nov.	comb. nov. [basonym: *Achromobacter aestuarii* Kim *et al.* 2021]
Species etymology	–	fra.xi'ne.a. L. fem. adj. *fraxinea*, of the ash tree	aes.tu.a'ri.i. L. gen. n. *aestuarii* of estuary, pertaining to source of isolation
Designation of the Type Strain	–	B3P038^T	KS-M25^T
Strain Collection Numbers	–	LMG 33092 ^{T}; DSM 115926 ^{T}	KACC 21219 ^{T}; JCM 33329 ^{T}
Type Genome	–	GCA_030849945.1	GCA_009866805.1
Genome status	–	Incomplete	Incomplete
Genome size	–	5,442 kbp	5,338 kbp
GC mol%	61.9–62.3	61.9	62.3
16S rRNA gene accession nr.	–	OR531683	MH651750
Description of the new taxon and diagnostic traits	Cells are Gram-stain-negative, non-spore-forming, motile, and rod-shaped. Q-8 is the predominant ubiquinone. The polyamine profile consists of putrescine and 2-hydroxyputrescine. The main cellular fatty acids are $C_{16:1}$ *ω7c*, $C_{16:0}$, $C_{18:1}$ *ω7c*.	General description are as for the genus. Rods are 0.6–1.0x1.6–2.3 μm. Colonies are creamy, opaque, and convex with entire margins after growth on TSA for 3 days at 25C. It is able to grow on TSA, Reasoner's 2A agar, nutrient agar and on MacConkey agar. Growth occurs at 4 to 30 °C (optimum 25–30 °C). No growth is observed at 35 °C. Cells can grow in NB at pH 5.0–10.0 (optimum pH 7.5) and at 0–6 % NaCl (optimum 0.5 % NaCl). Nitrate is not reduced. Strains are positive for catalase, oxidase, and aesculin hydrolyses but negative for gelatinase, tryptophane deaminase, ß-galactosidase, arginine dihydrolase, urease, lysine and ornithine decarboxylase. Production of indole, H_2S and acetoin is negative. Citrate utilization is weak. Adipic acid, malic acid, trisodium citrate, phenylacetic acid are assimilated in the API 20NE test stripes. In the Biolog GEN III Microplate assay following substrates are oxidized: D-fructose, D-fructose- 6-PO_4, D- and L-serine, L-alanine, L-aspartic acid, L-glutamic acid, D-galacturonic acid, D-gluconic acid, D-glucuronic acid, glucuronamide, D-saccharic acid, methyl pyruvate, L-lactic acid, citric acid, α-keto-glutaric acid, D- and L- malic acid, bromo-succinic acid, α-keto-butyric acid, and acetic acid. The strains are able to grow in the presence of 1 % sodium lactate, fusidic acid, troleandomycin, rifamycin SV, lincomycin, guanidine HCl, niaproof 4, vancomycin, nalidixic acid, lithium chloride, potassium tellurite, aztreonam, and sodium butyrate. Tetrazolium blue and tetrazolium violet are reduced. Strains react differently to D- and L-fucose, glycyl-L-proline, D-lactic acid methyl ester, α-hydroxy butyric acid, and acetoacetic acid. No reactions are obtained for dextrin, D-maltose, D-trehalose, D-cellobiose, gentiobiose, sucrose, D-turanose, stachyose, D-raffinose, α-D-lactose, D-melibiose, β-methyl-D-glucoside, D-salicin, *N*-acetyl-D-glucosamine, *N*-acetyl-β-D-mannosamine, *N*-acetyl-D-galactosamine, *N*-acetyl neuraminic acid, α-D-glucose, D-mannose, D-galactose, 3-methyl glucose, L-rhamnose, inosine, D-sorbitol, D-mannitol, D-arabitol, myo-inositol, glycerol, D-glucose-6-PO_4, D-aspartic acid, L-arginine, L-histidine, L-pyroglutamic acid, pectin, L-galactonic acid lactone, mucic acid, quinic acid, *p*-hydroxy-phenylacetic acid, tween 40, γ-amino-butryric acid, β-hydroxy-D,L butyric acid,	The characteristics of the species are as given by Kim et al. (2021). Additional characteristics from this study are as follows: In the Biolog GEN III Microplate assay following substrates are oxidized: D-fructose, D-fructose- 6-PO_4, D- and L-serine, L-alanine, L-aspartic acid, D- and L-fucose, L-glutamic acid, D-galacturonic acid, D-gluconic acid, D-glucuronic acid, glucuronamide, glycyl-L-proline, D-saccharic acid, methyl pyruvate, L-lactic acid, citric acid, α-keto-glutaric acid, D- and L- malic acid, bromo-succinic acid, α-keto-butyric acid, α-hydroxy butyric acid, acetoacetic acid, propionic acid and acetic acid. The strains are able to grow in the presence of 1 % sodium lactate, fusidic acid, troleandomycin, rifamycin SV, lincomycin, guanidine HCl, niaproof 4, vancomycin, nalidixic acid, lithium chloride, aztreonam, and sodium butyrate. Tetrazolium blue and tetrazolium violet are reduced. No reactions are obtained for dextrin, D-maltose, D-trehalose, D-cellobiose, gentiobiose, sucrose, D-turanose, stachyose, D-raffinose, α-D-lactose, D-melibiose, β-methyl-D-glucoside, D-salicin, *N*-acetyl-D-glucosamine, *N*-acetyl-β-D-mannosamine, *N*-acetyl-D-galactosamine, *N*-acetyl neuraminic acid, D-lactic acid methyl ester, α-D-glucose, D-mannose, D-galactose, 3-methyl glucose, L-rhamnose, inosine, D-sorbitol, D-mannitol, D-arabitol, myo-inositol, glycerol, D-glucose-6-PO_4, D-aspartic acid, L-arginine, L-histidine, L-pyroglutamic acid, pectin, L-galactonic acid lactone, mucic acid, quinic acid, *p*-hydroxy-phenylacetic acid, tween 40, γ-amino-butryric acid, β-hydroxy-D,L butyric acid, formic acid, minocycline, potassium tellurite, and sodium bromate. The polyamine profile consists of putrescine and 2-hydroxyputrescine, and the polar lipid patterns include diphosphatidylglycerol, phosphatidylethanolamine, phosphatidylglycerol, a phospholipid, a lipid, and an aminolipid.

(*continued on next page*)

Table 4 (*continued*)

Guiding Code for Nomenclature [req]	ICNP	ICNP	ICNP
		propionic acid, formic acid, minocycline, and sodium bromate. The polar lipids diphosphatidylglycerol, phosphatidylethanolamine, phosphatidylglycerol, aminophospholipid and a lipid are present in all strains. The presence of a phospholipid and an aminolipid was strain-specific. The cellular fatty acid profile consists of $C_{16:1}$ *ω7c*, $C_{16:0}$, $C_{18:1}$ *ω7c* (major components > 10 %) and $C_{14:0}$ 3-OH, $C_{14:0}$, $C_{18:0}$, $C_{12:0}$, $C_{17:0}$, $C_{12:0}$ 2-OH, $C_{12:0}$ 3-OH (minor components > 0.5 %).	
Country of origin	–	Germany	South Korea
Region of origin	–	Mecklenburg-Vorpommern	Gunsan, Jeollanam-do Geum river
Date of isolation	–	21/07/2017	–
Source of isolation	–	compound leaves of *Fraxinus excelsior*	estuary water
Sampling date	–	20/07/2017	–
Latitude	–	54°15′25.9″N	–
Longitude	–	12°52′12.5″E	–
Number of strains in study	–	3	–
Source of isolation of non-type strains	–	compound leaves of *Fraxinus excelsior*	–
Information related to the Nagoya Protocol	Country profile: https://absch.cbd.int/countries/DE; Party to Nagoya as of: 20–07-2016	Country profile: https://absch.cbd.int/countries/DE; Party to Nagoya as of: 20–07-2016	–

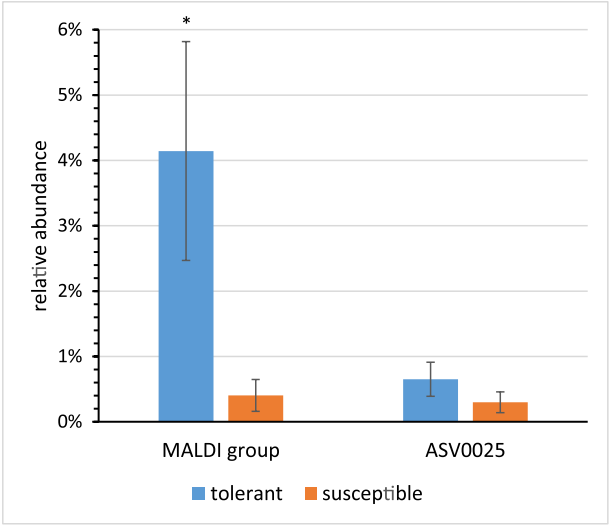

Fig. 6. Proportion of *Schauerella fraxinea* in the bacterial microbiome of ash leaves from tolerant and susceptible trees, as determined by MALDI-group classification and amplicon sequencing (ASV0025).

± 1.0 %) and *S. aestuarii* (9.1 %), indicating variations at the species level (Table 2). Furthermore, the presence of the hydroxylated fatty acid $C_{14:0}$ 2-OH in the species *S. aestuarii* allowed for differentiation from *S. fraxinea*. Physiological characterisation of the isolated strains and *S. aestuarii* JCM 33329 ^{T} revealed consistency in a large number of traits. Nevertheless, some characteristics were found that allow delimitation (Table 3). In particular, differences were observed in the utilization of various carbohydrates in the Biolog GEN III assay. A detailed description of the *Shauerella fraxinea* gen. nov., sp. nov. (B3P038^{T}) is provided in the protologue (Table 4).

Ecological significance

Colonisation of ash trees in relation to their tolerance against ash dieback. Analyses of the leaf microbiome in four ash stands exposed to *H. fraxineus* revealed several bacterial groups with significantly higher abundance in tolerant trees (Becker et al., 2022; Ulrich et al., 2020; Ulrich et al., 2022). The investigated strains were isolated from these sites and represent one of the specific groups. A total of 70 isolates constituted this group based on classification by MALDI-TOF MS, with 92.9 % of them being isolated from tolerant ash trees. The relative abundance of this group, comprising 4.1 % of the entire cultured bacterial community, is significantly higher than the 0.4 % found on susceptible trees (Fig. 6). A comparable result, albeit less distinct, was obtained for the corresponding amplicon sequence variant (ASV0025) determined by amplicon sequencing of the 16S rRNA gene. The abundance was increased 2-fold in the tolerant trees (Fig. 6). These findings suggest that the members of the species *S. fraxinea* might contribute to the resilience of trees against the pathogen *H. fraxineus*. Hence, the isolated strains are interesting for further investigations to assess their potential as inoculants for the containment of the pathogenic fungus. Promising are the results obtained so far for representatives of individual groups, which were also predominantly found on tolerant ash trees (Becker et al., 2022; Ulrich et al., 2022). Thus, inoculation experiments on ash seedlings demonstrated the plant health-protecting effect of strain *Luteimonas fraxinea* D4P002^{T} and *Aureimonas altamirensis* C2P003, which were accompanied by a shift in the leaf microbiome. It is assumed that *H. fraxineus* was suppressed either by colonisation resistance or indirectly through changes in the microbiome composition.

To assess the extent to which potential members of the new species *S. fraxinea* are distributed and in which habitats they may still be found, a screening was conducted in public databases. A total of 9 isolates could be identified with a 16S rRNA gene sequence similarity higher than 98.65 %. These isolates mostly originate from samples of plant origin and soil. In contrast, the search based on housekeeping genes yielded no results. Interesting results could be obtained from the analysis of amplicon sequencing data of the microbiome of ash leaves at different stands in the UK (Griffiths et al., 2020). At one site out of the 137 different locations, an ASV with almost identical 16S rRNA gene

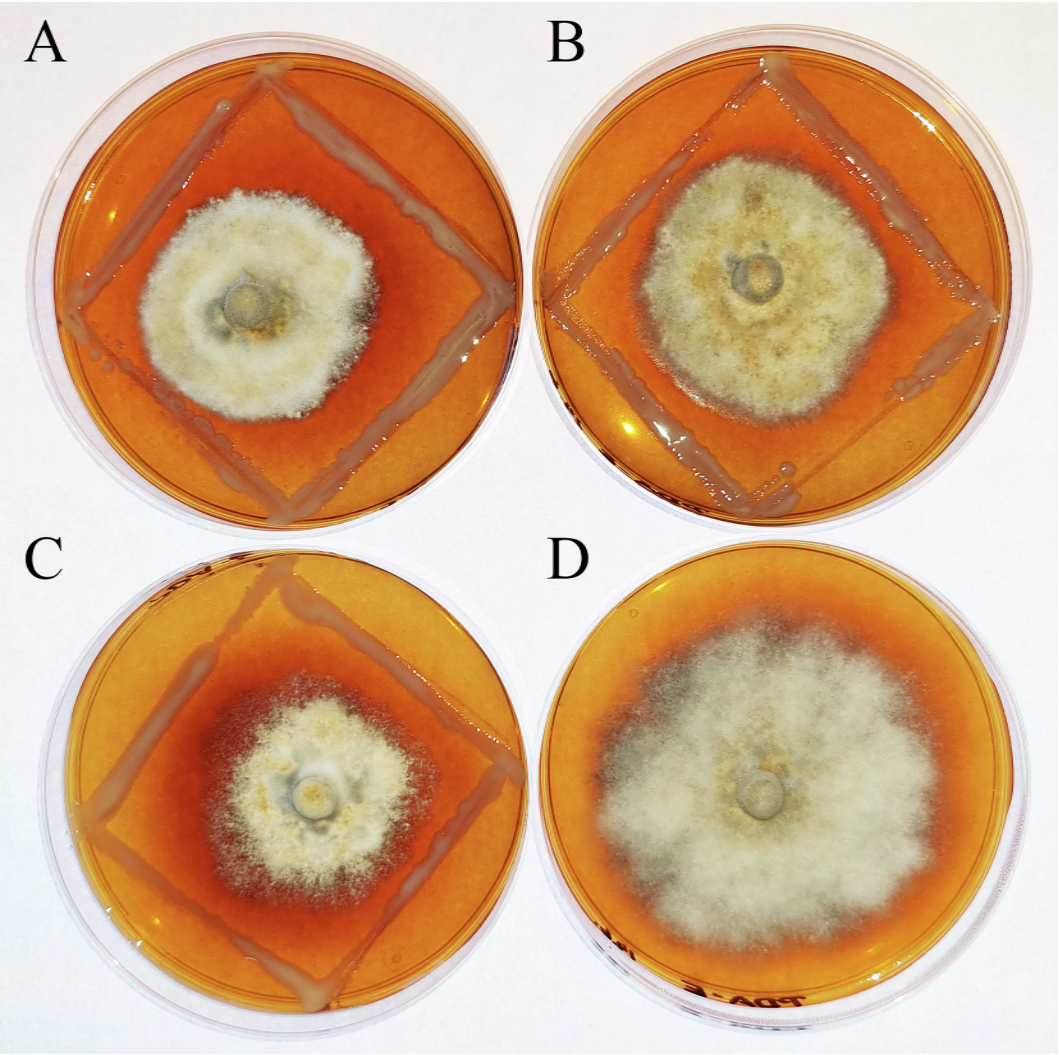

Fig. 7. Inhibition of *H. fraxineus* 7 growth by co-cultivation with *S. fraxinea* strain C4P045 (A), A4P071 (B), and B3P038^T (C). The growth of *H. fraxineus* 7 without co-cultivation served as the control (D).

sequence could be revealed (similarity of 99.6 %). The relative abundance of this ASV in the microbiome of ash leaves was 0.20 %. This result indicated a special association of *S. fraxinea* with ash leaves.

Antagonistic potential in the growth inhibition test. The isolated strains were screened for their potential to inhibit the growth of three different *H. fraxineus* strains in a co-cultivation assay. All strains significantly restricted the growth of strain *H. fraxineus* 7 compared to the control (Fig. 7). The growth limitation can be considered moderate, with the most significant impact observed for strain B3P038^T. In contrast, no inhibition could be demonstrated in the growth of *H. fraxineus* strains HF6 and HF8. This result indicates that the strains have antagonistic potential *in vitro* against some of the *H. fraxineus* stains. The ecological relevance should be tested with an inoculation experiment in a field trial.

Strain-specific qPCR assay for plant-colonisation studies. To provide a tool for the monitoring of colonisation and persistence of *S. fraxinea* B3P038^T, a strain-specific qPCR assay was designed and established. The genome of strain B3P038^T was compared to the 322 genomes available for the family *Alcaligenaceae*. In total, 84 specific sequence fragments were found within the genome of strain B3P038^T. The highest ranked sequence fragment had a length of 3689 bp and was used for the design of the Primer-Probe System. The amplicon with a length of 171 bp is located at position 869,557–869,727 of the genome sequence of B3P038^T (JAVDKK000000000). The specificity of the qPCR system was tested with bacterial strains that are closely related to the target strain (*S. fraxinea* C4P045 and *S. fraxinea* A4P071) and the type strain of *A. aestuarii* (JCM 33329 ^{T}). Only the target strain B3P038^T was detected, the other strains were undetectable. One copy of the target gene could be reliably detected (in two of the three replicates). The properties of this qPCR assay, which are comparable with similar detection systems (Burghard et al., 2023) are a good basis for a sensitive and specific detection of B3P038^T in plant material, to study inoculation success and persistence on or in ash leaves.

Genomic features associated with potential bacteria-pathogen interactions. A functional analysis of the annotated genome of strain B3P038^T was performed to reveal features putatively involved in its ability to suppress the growth of pathogenic fungi. Genes required for the biosynthesis of PABA (*para*-aminobenzoic acid) (Green et al., 1992), were found in the genome, including *pabA*, *pabB* and *pabC* (Table S2). PABA, a cyclic amino acid belonging to the vitamin B group, is known to be produced by bacteria, yeast and plants (Maki and Takeda, 2000). PABA secreted by the rhizobacterium *Lysobacter antibioticus* OH13 showed a broad spectrum of antifungal activities. Based on its effect on the fungal cell cycle, PABA was also proved to be effective in biocontrol of the bitter rot disease pathogen *Colletotrichum fructicola* in pears (Laborda et al., 2018; Laborda et al., 2019). In pepper seedlings, PABA mediated systemic acquired resistance against the bacterial leaf spot pathogen *Xanthomonas axonopodis* (Song et al., 2013).

Furthermore, a gene encoding the enzyme PhzF, catalyzing a key reaction in the biosynthesis of phenazines (Diederich et al., 2017; Liu et al., 2015), was detected. Phenazines show broad-spectrum bioactivities, such as antibiotic activities against bacteria, fungi and yeasts (Blankenfeldt et al., 2004).

The formation of putrescine is another interesting capability indicating potential antagonistic activity. The most prevalent route for the synthesis of the polyamine putrescine is mediated by the genes *speA* and *speB*. The arginine decarboxylase SpeA, which is usually required for the decarboxylation of arginine to agmatine could not be identified. In the strain B3P038^T, an alternative arginine decarboxylase (Table S2) appears to be responsible for this reaction. The agmatinase SpeB (Table S2) catalyzing the second step of the synthesis of putrescine was found in the genome. Polyamines play a significant role in various bacteria-plant interactions, resulting in growth promotion (Xie et al., 2014), protection against various environmental stresses, and the formation of biofilms and colonisation processes (McGinnis et al., 2009). Moreover, putrescine was shown to be involved in modulating plant defense. Song et al. (2023) demonstrated an antifungal activity against *Colletotrichum gloeosporioides* in *in vitro* tests which could effectively reduce the incidence rate and severity of anthracnose disease of mango fruits.

To determine if these features revealed for B3P038^T are also present in *S. fraxinea* A4P071, C4P045, and the type strain of *S. aestuarii*, these strains were also included in the analysis. The found features seems to be common within the genus *Schauerella*, as the corresponding genes could be detected in all strains.

Conclusions

The taxonomic analysis of a bacterial group associated with ash trees revealed that it constitutes a separate species in a new genus named *Schauerella fraxinea* sp. nov., gen. nov. This classification was demonstrated through a comprehensive phylogenomic study, based on the phylogeny of well-known marker genes and core orthologous genes within the family *Alcaligenaceae*. A detailed chemotaxonomic analysis complements the description of the new genus. Moreover, it was demonstrated that the related species *Achromobacter aestuarii* should be reclassified as a species of the new genus and renamed as *Schauerella aestuarii* comb. nov.

An increased occurrence of the studied group in the phyllosphere of ash trees tolerant to ash dieback, along with demonstrated antagonistic activity, suggests their involvement in protecting trees from dieback. The genetic makeup supports this assumption. For a planned inoculation under field conditions, a strain-specific qPCR assay was developed to establish an efficient method for monitoring inoculation success and persistence through specific quantification.

Funding information

This research received funding via the Waldklimafonds (WKF) funded by the German Federal Ministry of Food and Agriculture (BMEL) and Federal Ministry for the Environment, Nature Conservation, Nuclear Safety and Consumer Protection (BMUV) administrated by the Agency for Renewable Resources (FNR), grant number 2219WK22I4.

CRediT authorship contribution statement

Undine Behrendt: Writing – review & editing, Writing – original draft, Visualization, Investigation, Conceptualization. **Valentin Burghard:** Writing – review & editing, Formal analysis. **Sonja Wende:** Writing – review & editing, Formal analysis, Data curation. **Kristina Ulrich:** Writing – review & editing, Investigation, Formal analysis. **Jacqueline Wolf:** Writing – review & editing, Investigation. **Meina Neumann-Schaal:** Writing – review & editing, Investigation. **Andreas Ulrich:** Writing – review & editing, Visualization, Supervision, Project administration, Funding acquisition, Formal analysis, Conceptualization.

Data availability

Data will be made available on request.

Acknowledgements

We thank Darline Krebel Birgit Grün, Gesa Martens, Anja Frühling and Anika Wasner for providing excellent technical assistance and Regina Becker for helpful discussion. We would also like to thank Aharon Oren for reviewing the Latin name of the new taxon.

Appendix A. Supplementary data

Supplementary data to this article can be found online at https://doi.org/10.1016/j.syapm.2024.126516.

References

Abdel-Rahman, H.M., Salem, A.A., Moustafa, M.M.A., El-Garhy, H.A.S., 2017. A novice *Achromobacter* sp. EMCC1936 strain acts as a plant-growth-promoting agent. Acta Physiol. Plant. 39, 61.

Austin, B., 2014. The family *Alcaligenaceae*. In: Rosenberg, E., DeLong, E.F., Lory, S., Stackebrandt, E., Thompson, F. (Eds.), The Prokaryotes: Alphaproteobacteria and Betaproteobacteria. Springer, Berlin Heidelberg, Berlin, Heidelberg, pp. 729–757.

Aziz, R.K., Bartels, D., Best, A.A., DeJongh, M., Disz, T., Edwards, R.A., Formsma, K., Gerdes, S., Glass, E.M., Kubal, M., Meyer, F., Olsen, G.J., Olson, R., Osterman, A.L., Overbeek, R.A., McNeil, L.K., Paarmann, D., Paczian, T., Parrello, B., Pusch, G.D., Reich, C., Stevens, R., Vassieva, O., Vonstein, V., Wilke, A., Zagnitko, O., 2008. The RAST Server: rapid annotations using subsystems technology. BMC Genomics 9, 75.

Babich, T.L., Grouzdev, D.S., Sokolova, D.S., Tourova, T.P., Poltaraus, A.B., Nazina, T.N., 2023. Genome analysis of *Pollutimonas subterranea* gen. nov., sp. nov. and *Pollutimonas nitritireducens* sp. nov., isolated from nitrate- and radionuclide-contaminated groundwater, and transfer of several *Pusillimonas* species into three new genera *Allopusillimonas, Neopusillimonas*, and *Mesopusillimonas*. Antonie Van Leeuwenhoek 116, 109–127.

Baral, H.O., Queloz, V., Hosoya, T., 2014. *Hymenoscyphus fraxineus*, the correct scientific name for the fungus causing ash dieback in Europe. IMA Fungus 5, 79–80.

Barco, R.A., Garrity, G.M., Scott, J.J., Amend, J.P., Nealson, K.H., 2020. Emerson D. A genus definition for *Bacteria* and *Archaea* based on a standard genome relatedness index, mBio 11, e02475–02419.

Barta, M., Pastirčáková, K., Ostrovský, R., Kobza, M., Kádasi, H.M., 2022. Culturable endophytic fungi in *Fraxinus excelsior* and their interactions with *Hymenoscyphus fraxineus*. Forests 13, 1098.

Becker, R., Ulrich, K., Behrendt, U., Schneck, V., Ulrich, A., 2022. Genomic characterization of *Aureimonas altamirensis* C2P003 - A specific member of the microbiome of *Fraxinus excelsior* trees tolerant to ash dieback. Plants 11, 3487.

Behrendt, U., Ulrich, A., Schumann, P., Erler, W., Burghardt, J., Seyfarth, W., 1999. A taxonomic study of bacteria isolated from grasses: a proposed new species *Pseudomonas graminis* sp. nov. Int. J. Syst. Bacteriol. 49, 297–308.

Behrendt, U., Wende, S., Kolb, S., Ulrich, A., 2019. Genome-based phylogeny of the genera *Proteus* and *Cosenzaea* and description of *Proteus terrae* subsp. *terrae* subsp. nov. and *Proteus terrae* subsp. *cibarius* subsp. nov. Int. J. Syst. Evol. Microbiol. 71.

Bilański, P., Kowalski, T., 2022. Fungal endophytes in *Fraxinus excelsior* petioles and their in vitro antagonistic potential against the ash dieback pathogen *Hymenoscyphus fraxineus*. Microbiol. Res. 257, 126961.

Blankenfeldt, W., Kuzin, A.P., Skarina, T., Korniyenko, Y., Tong, L., Bayer, P., Janning, P., Thomashow, L.S., Mavrodi, D.V., 2004. Structure and function of the phenazine biosynthetic protein PhzF from *Pseudomonas fluorescens*. Proc Natl Acad Sci U S A 101, 16431–16436.

Bligh, E.G., Dyer, W.J., 1959. A rapid method of total lipid extraction and purification. Can J Biochem Physiol 37, 911–917.

Buchfink, B., Xie, C., Huson, D.H., 2015. Fast and sensitive protein alignment using DIAMOND. Nat. Methods 12, 59–60.

Burghard, V., Wende, S., Ulrich, A., 2023. Strain-specific quantitative detection of two putative biocontrol strains for suppression of ash dieback. Biol. Control 187, 105376.

Busse, H.-J., Stolz, A., 2006. *Achromobacter*, *Alcaligenes* and related genera. In: Dworkin, M., Falkow, S., Rosenberg, E., Schleifer, K.-.-H., Stackebrandt, E. (Eds.), The Prokaryotes: Volume 5: Proteobacteria: Alpha and Beta Subclasses. Springer, New York, New York, NY, pp. 675–700.

Chaumeil, P.-A., Mussig, A.J., Hugenholtz, P., Parks, D.H., 2022. GTDB-Tk v2: memory friendly classification with the genome taxonomy database. Bioinformatics 38, 5315–5316.

Conway, J.R., Lex, A., Gehlenborg, N., 2017. UpSetR: an R package for the visualization of intersecting sets and their properties. Bioinformatics 33, 2938–2940.

Deyett, E., Roper, M.C., Ruegger, P., Yang, J.-I., Borneman, J., Rolshausen, P.E., 2017. Microbial landscape of the grapevine endosphere in the context of Pierce's disease. Phytobiomes Journal 1, 138–149.

Diederich, C., Leypold, M., Culka, M., Weber, H., Breinbauer, R., Ullmann, G.M., Blankenfeldt, W., 2017. Mechanisms and specificity of phenazine biosynthesis protein PhzF. Sci. Rep. 7, 6272.
Dong, M., Yang Z., Cheng G., Peng L., Xu Q., Xu J., 2018. Diversity of the bacterial microbiome in the roots of four *Saccharum* species: *S. spontaneum*, *S. robustum*, *S. barberi,* and *S. officinarum*, Front. Microbiol., 9.
Edgar, R.C., 2010. Search and clustering orders of magnitude faster than BLAST. Bioinformatics 26, 2460–2461.
Emms, D.M., Kelly, S., 2019. OrthoFinder: phylogenetic orthology inference for comparative genomics. Genome Biol. 20, 238.
Enderle, R., Stenlid, J., Vasaitis, R., 2019. An overview of ash (*Fraxinus* spp.) and the ash dieback disease in Europe. CABI Reviews 1–12.
George, J.-P., Sanders, T.G.M., Timmermann, V., Potočić, N., Lang, M., 2022. European-wide forest monitoring substantiate the neccessity for a joint conservation strategy to rescue European ash species (*Fraxinus* spp.). Sci. Rep. 12, 4764.
Green, J.M., Merkel, W.K., Nichols, B.P., 1992. Characterization and sequence of *Escherichia coli* pabC, the gene encoding aminodeoxychorismate lyase, a pyridoxal phosphate-containing enzyme. J. Bacteriol. 174, 5317–5323.
Griffiths, S.M., Galambao, M., Rowntree, J., Goodhead, I., Hall, J., O'Brien, D., Atkinson, N., Antwis, R.E., 2020. Complex associations between cross-kingdom microbial endophytes and host genotype in ash dieback disease dynamics. J. Ecol. 108, 291–309.
Hahn, M.W., Pitt, A., Schmidt, J., Koll, U., Wolf, J., Whitman, W.B., Bodelier, P.L.E., Neumann-Schaal, M., 2022. *Zwartia hollandica* gen. nov., sp. nov., *Jezberella montanilacus* gen. nov., sp. nov. and *Sheuella amnicola* gen. nov., comb. nov., representing the environmental GKS98 (betIII) cluster. Int. J. Syst. Evol. Microbiol. 72.
Hañáčková, Z., Havrdová, L., Černý, K., Zahradnik, D., Koukol, O., 2017. Fungal endophytes in ash shoots–diversity and inhibition of *Hymenoscyphus fraxineus*. Balt. For. 23, 89–106.
Huerta-Cepas, J., Forslund, K., Coelho, L.P., Szklarczyk, D., Jensen, L.J., von Mering, C., Bork, P., 2017. Fast genome-wide functional annotation through orthology assignment by EggNOG-mapper. Mol. Biol. Evol. 34, 2115–2122.
Hyatt, D., Chen, G.-L., LoCascio, P.F., Land, M.L., Larimer, F.W., Hauser, L.J., 2010. Prodigal: prokaryotic gene recognition and translation initiation site identification. BMC Bioinform. 11, 119.
Kalyaanamoorthy, S., Minh, B.Q., Wong, T.K.F., von Haeseler, A., Jermiin, L.S., 2017. ModelFinder: fast model selection for accurate phylogenetic estimates. Nat. Methods 14, 587–589.
Kanehisa, M., Sato, Y., Kawashima, M., Furumichi, M., Tanabe, M., 2016. KEGG as a reference resource for gene and protein annotation. Nucleic Acids Res 44. D457 D62.
Kim, S.C., Chung, S.O., Lee, H.J., 2021. *Achromobacter aestuarii* sp. nov., isolated from an estuary. Curr. Microbiol. 78, 411–416.
Kim, D., Park, S., Chun, J., 2021. Introducing EzAAI: a pipeline for high throughput calculations of prokaryotic average amino acid identity. J. Microbiol. 59, 476–480.
Konstantinidis, K.T., Tiedje, J.M., 2005. Towards a genome-based taxonomy for prokaryotes. J. Bacteriol. 187, 6258–6264.
Konstantinidis, K.T., Tiedje, J.M., 2007. Prokaryotic taxonomy and phylogeny in the genomic era: advancements and challenges ahead. Curr. Opin. Microbiol. 10, 504–509.
Konstantinidis, K.T., Rosselló-Móra, R., Amann, R., 2017. Uncultivated microbes in need of their own taxonomy. ISME J. 11, 2399–2406.
Kowalski, T., 2006. *Chalara fraxinea* sp. nov. associated with dieback of ash (*Fraxinus excelsior*) in Poland. For. Pathol. 36, 264-270.
Kowalski, T., Bilański, P., 2021. Fungi detected in the previous year's leaf petioles of *Fraxinus excelsior* and their antagonistic potential against *Hymenoscyphus fraxineus*. Forests 12, 1412.
Laborda, P., Zhao, Y., Ling, J., Hou, R., Liu, F., 2018. Production of antifungal *p*-aminobenzoic acid in *Lysobacter antibioticus* OH13. J. Agric. Food Chem. 66, 630–636.
Laborda, P., Li, C., Zhao, Y., Tang, B., Ling, J., He, F., Liu, F., 2019. Antifungal metabolite p-aminobenzoic acid (pABA): mechanism of action and efficacy for the biocontrol of pear bitter rot disease. J. Agric. Food Chem. 67, 2157–2165.
Langer, G.J., Fuchs, S., Osewold, J., Peters, S., Schrewe, F., Ridley, M., Kätzel, R., Bubner, B., Grüner, J., 2022. FraxForFuture—research on European ash dieback in Germany. J. Plant Dis. Prot. 129, 1285–1295.
Li, W., O'Neill, K.R., Haft, D.H., DiCuccio, M., Chetvernin, V., Badretdin, A., Coulouris, G., Chitsaz, F., Derbyshire, M.K., Durkin, A.S., Gonzales, N.R., Gwadz, M., Lanczycki, C.J., Song, J.S., Thanki, N., Wang, J., Yamashita, R.A., Yang, M., Zheng, C., Marchler-Bauer, A., Thibaud-Nissen, F., 2021. RefSeq: expanding the Prokaryotic Genome Annotation Pipeline reach with protein family model curation. Nucleic Acids Res. 49. D1020 D8.
Liu, F., Zhao, Y.-L., Wang, X., Hu, H., Peng, H., Wang, W., Wang, J.-F., Zhang, X., 2015. Elucidation of enzymatic mechanism of phenazine biosynthetic protein PhzF using QM/MM and MD simulations. PLoS One 10, e0139081.
Maki, T., Takeda, K., 2000. Benzoic acid and derivatives. Ullmann's Encyclopedia of Industrial Chemistry 3.
Marinier, E., Zaheer, R., Berry, C., Weedmark, K.A., Domaratzki, M., Mabon, P., Knox, N. C., Reimer, A.R., Graham, M.R., Chui, L., Patterson-Fortin, L., Zhang, J., Pagotto, F., Farber, J., Mahony, J., Seyer, K., Bekal, S., Tremblay, C., Isaac-Renton, J., Prystajecky, N., Chen, J., Slade, P., Van Domselaar, G., 2017. Neptune: a bioinformatics tool for rapid discovery of genomic variation in bacterial populations. Nucleic Acids Res. 45, e159.
Martin, M., 2011. Cutadapt removes adapter sequences from high-throughput sequencing reads. Embnet.journal 17.
McGinnis, M.W., Parker, Z.M., Walter, N.E., Rutkovsky, A.C., Cartaya-Marin, C., Karatan, E., 2009. Spermidine regulates *Vibrio cholerae* biofilm formation via transport and signaling pathways. FEMS Microbiol. Lett. 299, 166–174.
Meier-Kolthoff, J.P., Göker, M., 2019. TYGS is an automated high-throughput platform for state-of-the-art genome-based taxonomy. Nat. Commun. 10, 2182.
Meier-Kolthoff, J.P., Auch, A.F., Klenk, H.-P., Göker, M., 2013. Genome sequence-based species delimitation with confidence intervals and improved distance functions. BMC Bioinf. 14, 60.
Meier-Kolthoff, J.P., Klenk, H.-P., Göker, M., 2014. Taxonomic use of DNA G+C content and DNA–DNA hybridization in the genomic age. Int. J. Syst. Evol. Microbiol. 64, 352–356.
Mohamadpoor, M., Amini, J., Ashengroph, M., Azizi, A., 2022. Evaluation of biocontrol potential of *Achromobacter xylosoxidans* strain CTA8689 against common bean root rot. Physiol. Mol. Plant Pathol. 117, 101769.
Nascimento, F.X., Glick, B.R., Rossi, M.J., 2021. Multiple plant hormone catabolism activities: an adaptation to a plant-associated lifestyle by *Achromobacter* spp. Env Microbiol Rep 13, 533–539.
Ngo, H.T.T., Yin, C.S., 2016. *Luteimonas terrae* sp. nov., isolated from rhizosphere soil of *Radix ophiopogonis*. Int. J. Syst. Evol. Microbiol. 66, 1920–1925.
Nguyen, L.T., Schmidt, H.A., von Haeseler, A., Minh, B.Q., 2015. IQ-TREE: a fast and effective stochastic algorithm for estimating maximum-likelihood phylogenies. Mol. Biol. Evol. 32, 268–274.
Overbeek, R., Olson, R., Pusch, G.D., Olsen, G.J., Davis, J.J., Disz, T., Edwards, R.A., Gerdes, S., Parrello, B., Shukla, M., Vonstein, V., Wattam, A.R., Xia, F., Stevens, R., 2014. The SEED and the rapid annotation of microbial genomes using subsystems technology (RAST). Nucleic Acids Res. 42. D206 D14.
Palmer, M., Steenkamp, E.T., Blom, J., Hedlund, B.P., Venter, S.N., 2020. All ANIs are not created equal: implications for prokaryotic species boundaries and integration of ANIs into polyphasic taxonomy. Int. J. Syst. Evol. Microbiol. 70, 2937–2948.
Raj, G., Shadab, M., Deka, S., Das, M., Baruah, J., Bharali, R., Talukdar, N.C., 2019. Seed interior microbiome of rice genotypes indigenous to three agroecosystems of Indo-Burma biodiversity hotspot. BMC Genomics 20, 924.
Rashad, E.M., Shaheen, D.M., Al-Askar, A.A., Ghoneem, K.M., Arishi, A.A., Hassan, E.S. A., Saber, W.I.A., 2022. Seed Endophytic Achromobacter sp. F23KW as a Promising Growth Promoter and Biocontrol of Rhizoctonia Root Rot of Fenugreek. Molecules 27, 5546.
Santana, M.M., Rosa, A.P., Zamarreño, A.M., García-Mina, J.M., Rai, A., Cruz, C., 2022. *Achromobacter xylosoxidans* and Enteromorpha intestinalis extract improve tomato growth under salt stress. Agronomy 12, 934.
Schlegel, M., Dubach, V., von Buol, L., Sieber, T.N., 2016. Effects of endophytic fungi on the ash dieback pathogen. FEMS Microbiol. Ecol. 92.
Shamsi, W., Kondo, H., Ulrich, S., Rigling, D., Prospero, S., 2022. Novel RNA viruses from the native range of *Hymenoscyphus fraxineus*, the causal fungal agent of ash dieback. Virus Res. 320, 198901.
Sheu, S.-Y., Chen, L.-C., Yang, C.-C., Carlier, A., Chen, W.-M., 2020. *Orrella amnicola* sp. nov., isolated from a freshwater river, reclassification of *Algicoccus marinus* as *Orrella marina* comb. nov., and emended description of the genus *Orrella*. Int. J. Syst. Evol. Microbiol. 70, 6381–6389.
Sigma-Aldrich Co. LLC., OligoArchitect™ Online, in, http://www.oligoarchitect.com/ShowToolServlet?TYPE=DPROBE, 2014.
Skovsgaard, J.P., Wilhelm, G.J., Thomsen, I.M., Metzler, B., Kirisits, T., Havrdová, L., Enderle, R., Dobrowolska, D., Cleary, M., 2017. Clark J., Silvicultural strategies for *Fraxinus excelsior* in response to dieback caused by *Hymenoscyphus fraxineus*. Forestry: an International Journal of Forest Research 90, 455–472.
Song, G.C., Choi, H.K., Ryu, C.M., 2013. The folate precursor para-aminobenzoic acid elicits induced resistance against Cucumber mosaic virus and *Xanthomonas axonopodis*. Ann. Bot. 111, 925–934.
Song, Y., Ren, Y., Xue, Y., Lu, D., Yan, T., He, J., 2023. Putrescine (1,4-Diaminobutane) enhances antifungal activity in postharvest mango fruit against Colletotrichum gloeosporioides through direct fungicidal and induced resistance mechanisms. Pestic. Biochem. Physiol. 195, 105581.
Tiley, A.M.M., O'Hanlon R., 2022. Living with the impact of ash dieback disease – Local mitigation practices against *Hymenoscyphus fraxineus* on the island of Ireland, Biology and Environment: Proceedings of the Royal Irish Academy, 122, 67-84.
Timsy, B.U., Ulrich, A., Foesel, B.U., Spanner, T., Neumann-Schaal, M., Wolf, J., Schloter, M., Horn, M.A., Kolb, S., 2022. Genomic evidence for two pathways of formaldehyde oxidation and denitrification capabilities of the species *Paracoccus methylovorus* sp. nov. Int. J. Syst. Evol. Microbiol. 72.
Tindall, B.J., Sikorski, J., Smibert, R.A., Krieg, N.R., 2007. Phenotypic characterization and the principles of comparative systematics. In: Methods for General and Molecular Microbiology 330–393.
Tkacz, A., Cheema, J., Chandra, G., Grant, A., Poole, P.S., 2015. Stability and succession of the rhizosphere microbiota depends upon plant type and soil composition. ISME J. 9, 2349–2359.
Ulrich, K., Ulrich, A., Ewald, D., 2008. Diversity of endophytic bacterial communities in poplar grown under field conditions. FEMS Microbiol. Ecol. 63, 169–180.
Ulrich, K., Becker, R., Behrendt, U., Kube, M., Ulrich, A., 2020. A comparative analysis of ash leaf-colonizing bacterial communities identifies putative antagonists of *Hymenoscyphus fraxineus*. Front. Microbiol. 11, 966.
Ulrich, K., Becker, R., Behrendt, U., Kube, M., Schneck, V., Ulrich, A., 2022. Physiological and genomic characterisation of *Luteimonas fraxinea* sp. nov., a bacterial species associated with trees tolerant to ash dieback. Syst. Appl. Microbiol. 45, 126333.
Vandamme, P., Sutcliffe, I., 2021. Out with the old and in with the new: time to rethink twentieth century chemotaxonomic practices in bacterial taxonomy. Int. J. Syst. Evol. Microbiol. 71.

Varghese, N.J., Mukherjee, S., Ivanova, N., Konstantinidis, K.T., Mavrommatis, K., Kyrpides, N.C., Pati, A., 2015. Microbial species delineation using whole genome sequences. Nucleic Acids Res. 43, 6761–6771.

Vasilinetc, I., Prjibelski, A.D., Gurevich, A., Korobeynikov, A., Pevzner, P.A., 2015. Assembling short reads from jumping libraries with large insert sizes. Bioinformatics 31, 3262–3268.

Vaz-Moreira, I., Figueira V., Lopes A.R., De Brandt E., Vandamme P., Nunes O.C., Manaia C.M., 2011. *Candidimonas nitroreducens* gen. nov., sp. nov. and *Candidimonas humi* sp. nov., isolated from sewage sludge compost, Int. J. Syst. Evol. Microbiol. 61, 2238-2246.

Vieira, S., Huber K.J., Neumann-Schaal M., Geppert A., Luckner M., Wanner G., Overmann J., 2021. *Usitatibacter rugosus* gen. nov., sp. nov. and *Usitatibacter palustris* sp. nov., novel members of *Usitatibacteraceae* fam. nov. within the order *Nitrosomonadales* isolated from soil, Int. J. Syst. Evol. Microbiol. 71.

Will, S.E., Henke, P., Boedeker, C., Huang, S., Brinkmann, H., Rohde, M., Jarek, M., Friedl, T., Seufert, S., Schumacher, M., Overmann, J., Neumann-Schaal, M., Petersen, J., 2019. Day and night: Metabolic profiles and evolutionary relationships of six axenic non-marine cyanobacteria. Genome Biol Evol 11, 270–294.

Xie, S.S., Wu, H.J., Zang, H.Y., Wu, L.M., Zhu, Q.Q., Gao, X.W., 2014. Plant growth promotion by spermidine-producing *Bacillus subtilis* OKB105. Mol Plant Microbe Interact 27, 655–663.

Ying, J.-J., Zhang S.-L., Huang C.-Y., Xu L., Zhao Z., Wu M., Sun C., 2019. *Algicoccus marinus* gen. nov. sp. nov., a marine bacterium isolated from the surface of brown seaweed *Laminaria japonica*, Arch. Microbiol. 201, 943-950.

Yoon, S.H., Ha, S.M., Lim, J., Kwon, S., Chun, J., 2017. A large-scale evaluation of algorithms to calculate average nucleotide identity. Anton. Leeuw. Int. J. G. 110, 1281–1286.

Yoon, S.H., Ha, S.M., Kwon, S., Lim, J., Kim, Y., Seo, H., Chun, J., 2017. Introducing EzBioCloud: a taxonomically united database of 16S rRNA gene sequences and whole-genome assemblies. Int. J. Syst. Evol. Microbiol. 67, 1613–1617.

Zech, H., Thole, S., Schreiber, K., Kalhöfer, D., Voget, S., Brinkhoff, T., Simon, M., Schomburg, D., Rabus, R., 2009. Growth phase-dependent global protein and metabolite profiles of *Phaeobacter gallaeciensis* strain DSM 17395, a member of the marine *Roseobacter*-clade. Proteomics 9, 3677–3697.

Zhang, J., Kobert, K., Flouri, T., Stamatakis, A., 2013. PEAR: a fast and accurate Illumina Paired-End reAd mergeR. Bioinformatics 30, 614–620.